Case Studies in Thermal Engineering 35 (2022) 102067

Contents lists available at ScienceDirect

Case Studies in Thermal Engineering

journal homepage: www.elsevier.com/locate/csite

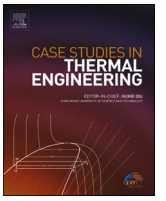

Thermodynamic analysis of general heat engine cycle with finite heat capacity rates for power maximization

Soyeon Kim [a], Young-Jin Baik [b], Minsung Kim [a,c,*]

[a] Department of Intelligent Energy and Industry, Chung-Ang University, 84 Heukseok-ro, Dongjak-gu, Seoul, 06974, Republic of Korea
[b] Thermal Energy Conversion Systems Laboratory, Korea Institute of Energy Research, 152 Gajeong-ro, Yuseong-gu, Dajeon, 34129, Republic of Korea
[c] School of Energy Systems Engineering, Chung-Ang University, 84 Heukseok-ro, Dongjak-gu, Seoul, 06974, Republic of Korea

ARTICLE INFO

Keywords:
Power maximization
Sequential carnot cycle
Waste heat recovery
Pattern search algorithm
Trilateral cycle

ABSTRACT

In this study, the ideal cycles with finite heat capacity rates is investigated theoretically to maximize power generation using a sequential Carnot cycle model. Although the Carnot efficiency is important, it is limited to evaluating only in terms of heat source/sink temperatures. For the actual heat engine, maximization of power generation is more important than cycle thermal efficiency when utilizing low-grade heat sources such as a waste heat. In this study, power generation optimization is numerically simulated under the fixed conditions of heat source temperatures, heat source flow rate and heat sink temperature. Effect by two design variables, compressor exit temperature and evaporator size ratio, were evaluated during cycle optimization. The optimization was performed using the pattern search algorithm (PSA) under a given thermal capacitance rate ratios and size of heat exchanger (*UA*) conditions. As a result, designing compressor exit temperature for maximizing the heat received from heat sources does not always maximize the power, but the higher the *UA* makes the optimum temperature lower, and the power output higher. These idealistic approaches can be useful in designing of cycle where the power maximization is crucial.

1. Introduction

To cope with energy and environmental issues, the government has been making efforts to promote the development, use, and distribution of new and renewable energy technologies, by providing policy support. In this regard, as low-grade renewable energy sources such as geothermal heat [1], solar heat [2], ocean temperature differences [3], and waste heat in non-volcanic regions have emerged recently, attempts have been made to use them to obtain electrical energy.

Research to convert thermal energy into electrical energy using a heat engine has been in progress for a long time, but most studies have focused on the steam Rankine cycle that uses combustion heat such as fossil fuel as a heat source. The aim has been to improve the efficiency of the first law of the cycle [4]. The heat source that has become cold after use is not reheated at a cost when using a renewable energy heat source, unlike the cycles using fossil fuels in the past. Other performance indicators such as the power that is actually produced are more important than focusing on the efficiency of the first law of the cycle.

These low-temperature heat sources convert energy using power cycles according to the temperature range. Among them, the supercritical carbon dioxide (sCO_2) cycle is identified as one of the technologies that can increase power generation efficiency in

* Corresponding author. Department of Intelligent Energy and Industry, Chung-Ang University, 84 Heukseok-ro, Dongjak-gu, Seoul, 06974, Republic of Korea.
E-mail address: minsungk@cau.ac.kr (M. Kim).

https://doi.org/10.1016/j.csite.2022.102067
Received 4 January 2022; Received in revised form 14 April 2022; Accepted 23 April 2022
Available online 27 April 2022

Nomenclature

A	heat transfer area [m^2]
$\dot{C}$	heat capacity [kJ/Ks]
c_p	specific heat [kJ/kgK]
HHV	higher heating value [kJ/kg]
$\dot{m}$	mass flow rate [kg/s]
N	number of micro Carnot cycles [−]
$\dot{Q}$	heat transfer rate [kJ/s]
s	entropy [kJ/kgK]
Δ	s relative entropy [kJ/kgK]
T	temperature [$^{\circ}C$, K]
Δ	T_{lm} log mean temperature difference [$^{\circ}C$]
U	overall heat transfer coefficient [kW/m^2K]
UA	size of heat exchanger [kW/K]
$UA_H/(UA_H + UA_L)$	evaporator size ratio [−]
$\dot{W}$	power (output work) [kW]

Greek symbol

η	efficiency

Subscripts

C	low-temperature side, cooling water
H	high-temperature side, heat source
h	high-temperature side in cycle
I	inlet condition of heat sources
i	element number of sequence cycle $(1, 2, \cdots,$ N$)$
L	low-temperature side, heat sink
l	low-temperature side in cycle
min	minimum
O	outlet condition of heat sources
th	thermal
1	cycle point at cooler outlet
2	cycle point at boiler inlet
3	cycle point at boiler outlet
4	cycle point at cooler inlet

Acronyms

CIT	compressor inlet temperature
CSP	concentrated solar power
Opt	optimum
ORC	Organic Rankine cycle
PSA	pattern search algorithm
TIT	turbine inlet temperature
sCO_2	supercritical carbon dioxide
WHR	waste heat recovery

several renewable energy fields such as nuclear power, thermodynamic analysis in concentrated solar power (CSP) [5,6], geothermal [7], and waste heat recovery systems (WHR) [8]. However, there are few discussions on waste heat itself in the studies, so WHR is not clearly defined.

Until now, the index for the performance of a heat engine with different types of heat source, especially the definition of the performance comparison of a cycle for a heat source with finite heat capacity, is unclear. In this study, the performance evaluation indexes of the heat engine, the cycle thermal efficiency and power capacity, are clarified by comparing the ideal cycles. It is purely idealistic and is developed through academic mathematical calculation.

To maximize the output of a power cycle driven by a heat source of finite heat capacity, Ondrechen et al. [9] proposed a sequential Carnot cycle model consisting of infinite micro Carnot cycles. The theoretical maximum output of the heat engine for a given heat source inlet condition was obtained under the conditions of a heat exchanger of infinite size and a heat sink of infinite heat capacity. Subsequently, Ibrahim et al. [10] and Ibrahim and Klein [11] argued that there is no analytic solution to obtaining the theoretical maximum output of a heat engine with a heat source and heat sink of a finite heat capacity, but that a numerical analysis solution can

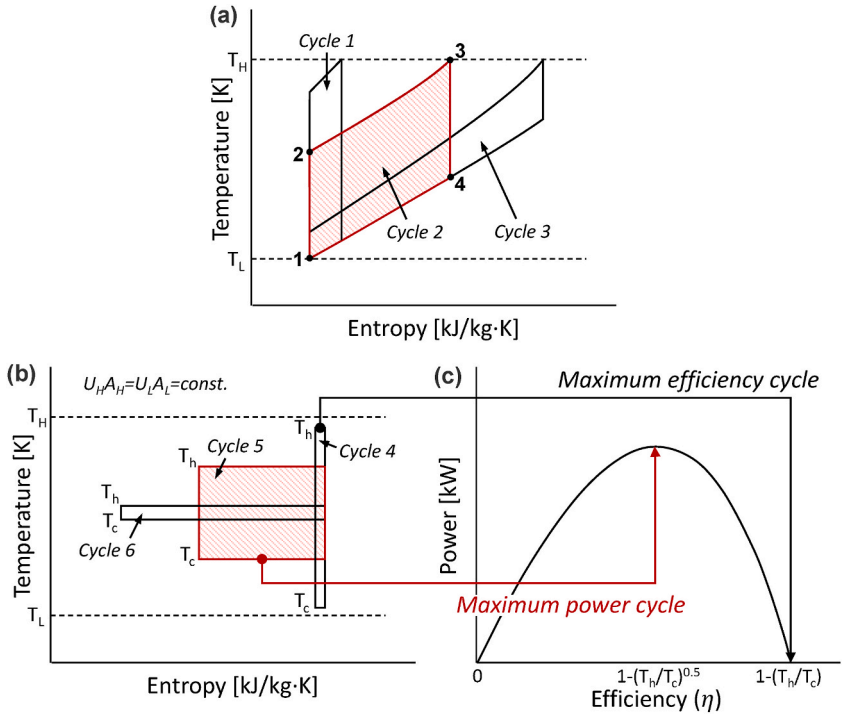

Fig. 1. Trade-off between power and efficiency and the ideal trilateral cycle [21].

be obtained using a sequential Carnot cycle model. However, discussions on the practical calculation process such as design variables and optimization methods of the model, and considerations on the change in characteristics of cycles due to changes in design conditions have not been sufficient.

Park and Kim (2014) [12] derived the performance of a cycle using a sequential Carnot cycle with a finite heat source and infinite heat sink using basic equations of thermodynamics and heat transfer. Numerical simulation of the organic Rankine cycle (ORC) was conducted based on design variables with finite heat source and sink, confirming that the sequential ORC has higher efficiency and increased work output than a single ORC [13]. However, both studies have not been sufficient to analyze changes in design variables with changes in cycle conditions.

The purpose of this study is to determine the theoretical maximum output of a heat engine based on the sequential Carnot cycle model using a low-grade heat source at approximately 100 °C given the conditions of the heat source and heat sink (coolant) flow rate. In addition, we determine the size of heat exchanger (*UA*) required for cycle operation, and consider changes in the value of the optimal design variables as the conditions change. These considerations can be used as a reference for the design and optimal operation of the actual low-grade heat source power cycle in the future.

Unlike previous studies [9–11], Baik et al. [4] maximized the output of the sequential Carnot cycle, through the optimization of two design variables using the pattern search algorithm (PSA) [14] in the MATLAB toolbox [15]. The change in the maximum power and values of the optimum design variables in the cycle according to the change in the *UA* which represents a size of heat exchanger over a wide range was also considered. This study covers all aspects of that study [4] and includes a theoretical approach to the ideal heat engine performance.

2. Heat engine with finite heat capacity rate

In the analysis of different heat engines that generate power, usually the cycle thermal efficiency (η_{th}) is used as the performance index and following basic thermodynamic relations for a cycle as below:

$$\eta_{th} = \frac{\dot{W}}{\dot{Q}_{in}} \tag{1}$$

$$\dot{Q}_{in} = \dot{m}c_p\Delta T = \dot{m}c_p(T_{HI} - T_{HO}) \tag{1-1}$$

$$\dot{Q}_{in} = \mathrm{HHV} \tag{1–2}$$

$$\dot{Q}_{in} = \chi = \dot{m}c(T_{HI} - T_{CI}) \tag{1–3}$$

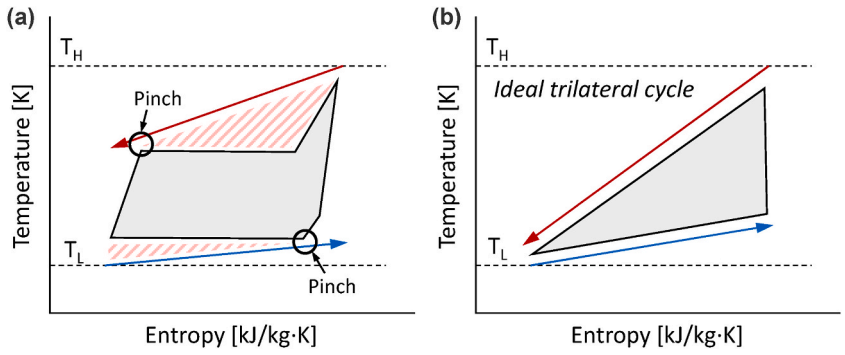

Fig. 2. Trade-off between power and efficiency and the ideal trilateral cycle [21].

In nuclear power plant, the primary fluid called as heat source in cycle returns to reactor after supply heat to cycle and it is reheated for heat exchange with cycle again. In this case, the amount of heat that supply to the working fluid from heat source (equations (1)–(1)) is input to $\dot{Q}_{in}$ in equation (1). In coal fired power plant, because the heat source (combusted hot air) is left the heat exchanger to atmosphere not circulated, the higher heating value (HHV) is used for thermal efficiency (equations (1) and (2)) based on 25 °C. Also in the case of low-grade heat source (waste heat), the heat source is not reheated, so the temperature difference between heat source and heat sink (equations (1)–(3)) is input to $\dot{Q}_{in}$ that means maximum of supply heat. χ is defined as the ratio of the thermal power absorbed by the bottoming cycle to total net recoverable thermal power. Heo et al. (2017) [16] suggested the performance indicator (practical index) for optimizing the heat recovery cycle called the waste heat recovery index (WHRI) by multiplying the cycle efficiency (η) by the heat recovery factor (χ). The WHRI means the ratio of the network generated by the bottoming cycle to total net thermal power recoverable due to thermal power. Ham et al. (2019) [17] evaluated the performance of the sCO_2 WHR system using the WHRI in a nuclear power plant application. Concepts such as the WHRI are also used in geothermal power plants, and Zarrouk and Moon (2014) [18] defined the power conversion efficiency and the actual efficiency as indexes to evaluate the performance according to the type of plant and they maximized the power through an exergy analysis.

In summary, the waste heat is discarded after heat exchange at evaporator, and the temperature and flow rate of waste heat is fixed (the heat capacity is fixed). So, the cycle design is important to use the heat as much as possible [19], and the power generation ($\dot{W}$) is more crucial performance index than thermal efficiency (η_{th}).

The discussion of performance index depends on the focus of η_{th} or power capacity relative to the actual heat engine characteristic. When optimizing the cycle, usually the gas power cycle (Brayton cycle) is an open cycle where the compressor inlet temperature (CIT) is constant at ambient temperature, and the turbine inlet temperature (TIT) is set as a metalogical limit. As the TIT and CIT are fixed, the closed Brayton cycle is structured as shown in Fig. 1 (a). In the concept of Carnot efficiency (equation (2)) or equation (1) when $\dot{Q}_{in} = \dot{m}c\Delta T$ (in equation (3)), cycle 1 has the best η_{th}, but it is known that the ideal Brayton cycle shows the best performance as power is maximized when T_2 and T_4 are the same [20].

$$\eta_{Carnot} = 1 - \frac{T_L}{T_H} \tag{2}$$

$$\dot{Q}_{in} = \dot{m}c\Delta T = UA\Delta T_{lm} \tag{3}$$

It is well known that the maximum efficiency that can be obtained between two constant temperature heat sources is the Carnot efficiency, and in many cases, this is considered the ideal efficiency that can be obtained from an actual heat engine. The ideal Carnot cycle does not consider the irreversibility of heat transfer, but since the finite temperature differences exist undoubtedly at the actual cycle point, so it must be defined differently from the Carnot cycle as shown in cycles 4–6 of Fig. 1 (b). According to equation (3), when the heat exchanger size (UA) is constant, using a low mass flow rate of working fluid ($\dot{m}$) reduces the total amount of heat received ($\dot{Q}_{in}$), so the temperature difference between the cycle and the heat source (ΔT_{lm}, irreversibility) in the heat exchanger can be reduced. In this Carnot efficiency concept, cycle 4 has the best performance in Fig. 1 (b), but at this time, the power generation ($\dot{W}$) corresponding to the area of the closed cycle approaches 0, and the η_{th} decreases. Rather, the maximum power is generated in cycle 5, which has the largest closed cycle area on the T-s diagram with an appropriate compression ratio [22]. So, the discussions depend on the focus of η_{th} or power capacity relative to the actual heat engine performance. In the case of waste heat, the power capacity must be maximized because it is discarded heat after being used, and in the case of nuclear and CSP, the concept of cycle 1 that can reduce the temperature difference between the heat source and cycle is more appropriate because the primary fluid is circulated and returned to cycle again after heat exchange [23].

As shown in Fig. 2 (a), in the case of the Rankine cycle, the irreversibility increases due to the pinch problem with the phase change of the working fluid, and the most ideal cycle in the finite heat capacity model is the ideal trilateral cycle [24] in Fig. 2 (b) [25]. In this study, the power is maximized with a sequential Carnot cycle model under the condition of a heat source with finite heat capacity. Since there is a finite temperature difference (irreversibility) in reality, the cycle where the power is maximized is optimized in the form of a trapezoid rather than an ideal trilateral cycle.

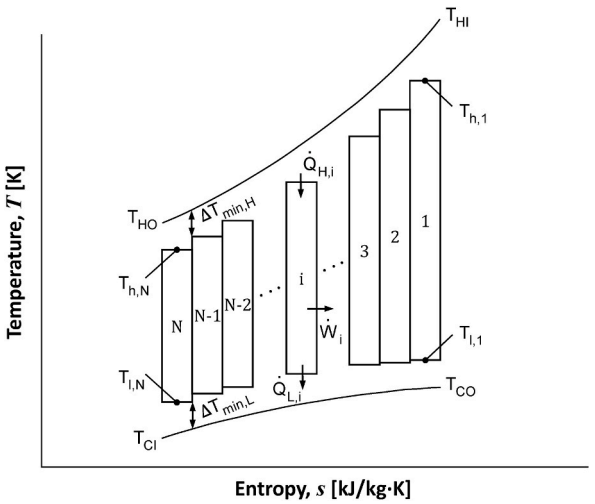

Fig. 3. Theoretical ideal cycle with finite heat capacity rates for the heat source and sink [21].

3. Cycle analysis

3.1. Cycle modeling

This study is based on the sequential Carnot cycle model [9–11], which is known to be able to obtain the theoretical maximum output of a heat engine under conditions of a heat source and sink (coolant) of a finite heat capacity as shown in Fig. 3 as a T-s diagram.

The *N*-sequential Carnot cycle can be thought of as a combination of *N* micro Carnot cycles, with the Carnot cycle consisting of two isothermal processes and two adiabatic processes corresponding to the case of $N = 1$. The output power ($\dot{W}$) of the *N*-sequential Carnot cycles in which the heat capacity of the heat source ($\dot{C}_H$) and the heat capacity of the heat sink ($\dot{C}_L$) are driven under a given condition is:

$$\dot{W} = \sum_{i=1}^{N} \left[\dot{Q}_{H,i} - \dot{Q}_{L,i}\right] = \sum_{i=1}^{N} \left[UA_{H,i}\,\Delta T_{lm,H,i} - UA_{L,i}\,\Delta T_{lm,L,i}\right] \tag{4}$$

Here, $UA_{H,i}$ and $\Delta T_{lm,H,i}$ denote the overall heat transfer coefficient and the logarithmic mean temperature difference (LMTD), respectively, required for the i-th micro Carnot cycle to receive heat from a heat source. Since each micro Carnot cycle is internally reversible, equation (5) holds:

$$\frac{\dot{Q}_{H,i}}{T_{H,i}} = \frac{\dot{Q}_{L,i}}{T_{L,i}} \tag{5}$$

In this study, two factors are chosen to optimize the output of the N-sequential Carnot cycles. The first factor is the high-temperature part of the *N*-th Carnot cycle ($T_{h,N}$) which means the compressor exit temperature, and the other is $UA_H/\ (UA_H + UA_L)$, which indicates the evaporator size ratio required to receive heat from the heat source among the overall heat transfer coefficient driving the cycle. The two design variables consist of conditions to be considered when constructing the actual cycle. $UA_H/(UA_H + UA_L)$ is an important parameter that affects the size and cost of a heat exchanger, and $T_{h,N}$ affects the design of the compressor.

For the convenience of calculation, we assume that the amount of heat received by each micro cycle ($\dot{Q}_{H,i}$) was the same, the minimum temperature difference between the micro cycles and the heat source is $\Delta T_{min,H}$, and that between the micro cycles and the heat sink is $\Delta T_{min,L}$.

As design conditions (heat source and heat sink inlet temperature, $\dot{m}$, and *UA*) are determined, the cycle output can be obtained by the process as shown in Fig. 4 given the above two design variables ($T_{h,N}$ and $UA_H/(UA_H + UA_L)$).

Unlike a general thermal power plant, waste heat is not reheated at a cost, so the amount of heat received cannot be controlled. Accordingly, the heat source inlet temperature (T_{HI}) and the flow rate of the heat source ($\dot{m}_H$) are fixed as boundary conditions. The temperature of the heat sink is generally set at ambient temperature, but the flow rate is fixed to several specific values. When the flow rate of the heat sink is infinite, the size of the heat exchanger (*UA*) is infinitely big, so it must be set as a boundary condition. The important research background in this study is that heat sources such as waste heat or geothermal heat cannot be set to a specific temperature and heat capacity at will. Therefore, to derive the maximum power from a finite heat capacity, it must be optimized to be close to the shape of the ideal trilateral cycle.

3.2. Methodology for cycle analysis

First, the minimum temperature difference in the heat exchanger of the hot part $\Delta T_{min,H}$ is assumed. The heat source outlet temperature $T_{HO,N}$ is obtained from the given $T_{h,N}$. By calculating the amount of heat $\dot{Q}_{H,N}$ of the *N*-th cycle and the LMTD $\Delta T_{lm,H,N}$ in the

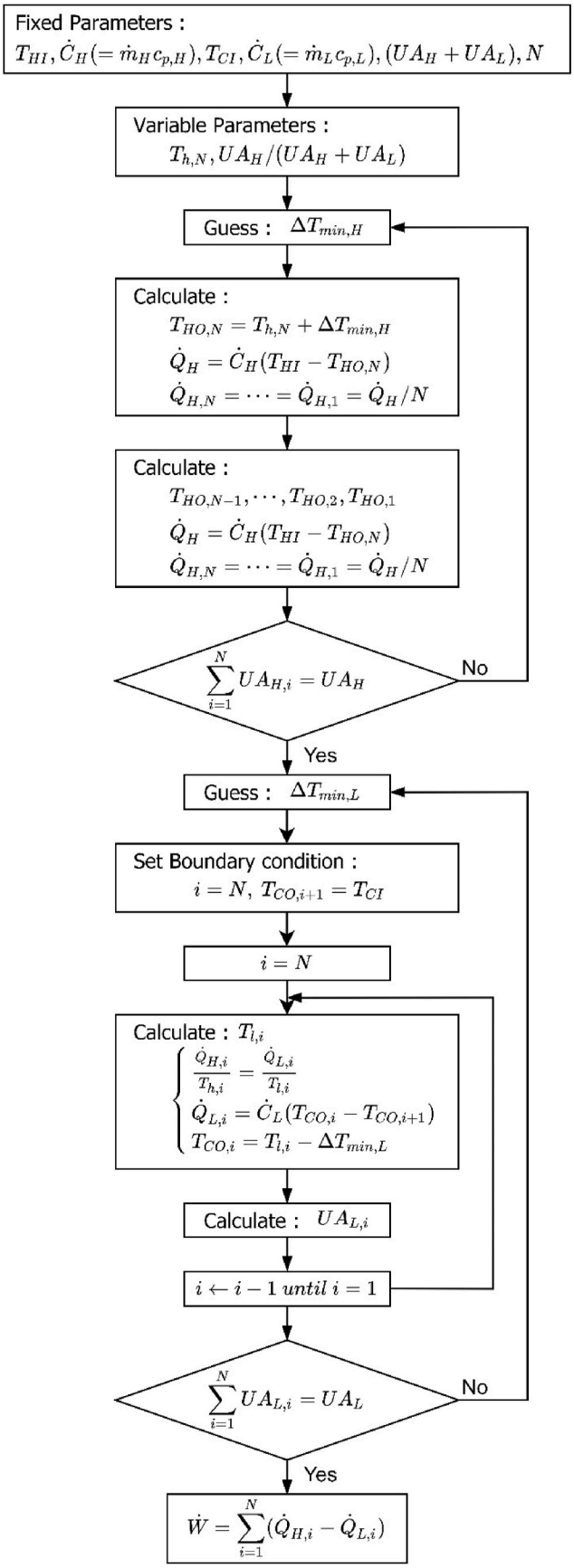

(caption on next page)

Fig. 4. Calculation procedure.

process of receiving heat, the $UA_{H,N}$ of the part receiving heat can be obtained. By repeating this process N-1, N-2, …, until the first cycle, the UA required for the N-sequential Carnot cycles ($\sum_{i=1}^{N} UA_{H,i}$) to receive heat can be obtained. If it is different from the given UA_H, $\Delta T_{min,H}$ is assumed again and the above process is repeated. If the condition $\sum_{i=1}^{N} UA_{H,i} \approx UA_H$ is satisfied, the minimum temperature difference $\Delta T_{min,L}$ in the heat exchanger of the low-temperature part is assumed. By solving the simultaneous equation (6) below, the low-temperature part temperature of the N-th cycle $T_{l,N}$ can be obtained.

$$\begin{cases} \dfrac{\dot{Q}_{H,i}}{T_{H,i}} = \dfrac{\dot{Q}_{L,i}}{T_{L,i}} \\ \dot{Q}_{L,i} = \dot{C}_L\left(T_{CO,i} - T_{CO,i+1}\right) \\ T_{CO,i} = T_{l,i} - \Delta T_{min,L} \end{cases} \tag{6}$$

The first relation of equation (6) should be satisfied with the Carnot cycle, and the second equation is used to obtain the rate of heat absorbed. The temperature of the heat sink $T_{CO,i}$ is obtained by the third equation using the given condition that the minimum temperature difference between the micro cycles and the heat sink is $\Delta T_{min,L}$ and is the boundary condition of the N-th cycle.

Using the temperature of the N-th cycle $T_{l,N}$, the above process is repeated for i set to N-1, N-2, …, 1, and then the UA can be obtained. If the calculated overall heat transfer coefficient $\sum_{i=1}^{N} UA_{L,i}$ required for heat released in the N-sequential Carnot cycles is different from the given UA_L, $\Delta T_{min,L}$ is assumed again and the above process is repeated. When the $\sum_{i=1}^{N} UA_{L,i} \approx UA_L$ condition is satisfied, the iteration ends, and the output of the cycle is obtained.

In this study, set $N = 100$, and the heat source inlet temperature (T_{HI}) and flow rate ($\dot{m}_H$) are fixed at 100 °C and 1 kg/s, respectively. Also, the heat sink (cooling water) inlet temperature T_{CI} is fixed at 20 °C. Under the above constraints, the output power is optimized by changing the overall heat transfer coefficient required for cycle driving ($UA_H + UA_L$) = 10–200 kW/K, and the heat sink flow rate ($\dot{m}_L$) is between 3 kg/s and 10 kg/s. Here, the flow rate of cooling water is determined by considering that the thermal capacitance rate ratio of the plant is generally between 3 and 10 [11,26,27].

4. Simulation result

For the first design variable $T_{h,N}$, the compressor exit temperature in the sequential Carnot cycles is related to the heat absorbed rate ($\dot{Q}_H$) and the finite temperature difference of the cycle. If $T_{h,N}$ is too high, the heat absorbed rate $\dot{Q}_H$ decreases and the output power cannot increase, whereas if it is too low, the heat absorbed rate $\dot{Q}_H$ is high, but the temperature difference between the heat source and the cycle increases to transfer a large amount of heat. Fig. 5 (a) shows the cycle T-s diagram for $T_{h,N} = 80$ °C ($\dot{W} = 14.4$ kW) where $T_{h,N}$ is too high for the optimal value. Fig. 5 (b) shows the cycle T-s diagram for $T_{h,N} = 26$ °C ($\dot{W} = 26.3$ kW) where $T_{h,N}$ is too low for the optimal value. The horizontal axis is the relative entropy (Δs) which defined as the change of entropy in the cycle with point 3 as the reference entropy. In contrast, if the evaporator size ratio ($UA_H/(UA_H + UA_L)$), which is the second design variable, is too high or too low compared to the optimal value, the temperature of the condenser increases or that of the evaporator decreases and the output power decreases, so that an optimal design value exists. This means that the lower the value of $T_{h,N}$, the closer the output is to the ideal trilateral cycle, but if it is too low or $UA_H/(UA_H + UA_L)$ is too high, the temperature of cycle point 1 (compressor inlet temperature, $T_{l,N}$) becomes higher than that of cycle point 2 (compressor outlet temperature, $T_{h,N}$) and the power decreases. In this case, since it cannot be said to be an ideal cycle, and power is not derived.

Since there are optimal values for both design variables for power maximization, to derive the optimal combination of these variables, the power contour map is shown at the flow rate of cooling water $\dot{m}_L = 10$ kg/s, and the size of heat exchanger (the sum of overall heat transfer coefficient, ($UA_H + UA_L$)) is fixed as 100 kW/K. As shown in Fig. 6, an optimal combination of two design variables exists to maximize the power. As Fig. 5 (c) shows, where compressor inlet temperature T_1 ($T_{l,N}$) is higher than outlet T_2 ($T_{h,N}$) is said to be a pinch and is represented as a pinched zone in Fig. 6.

As mentioned above, to maximize the output, it is necessary to find the optimal combination of the two design variables. For that, the PSA [14,15] is used in this study. PSA is one of the methods that can be used to solve the optimization problem of a multivariate function and has the advantage that it can be applied without information about the gradient of the objective function. In this study, the PSA is implemented using the Global Optimization Toolbox in the MATLAB [15] environment. In the PSA algorithm, each iteration is divided into *search phase* and *poll phase*. For each search phase, the objective function value is calculated at finite points on a mesh and find the mesh point which yields a lower value than that on current point. If there is a any lower point on mesh, it means the iteration is successful. The mesh size is doubled, and the process is reiterated. If the iteration is unsuccessful, the process refines the finer mesh than current, and the mesh points be polled to find if any lower function value [28].

The objective function of the PSA is the cycle output power $\dot{W}$, and the PSA function is to find the optimal combination of the two design variables that can maximize $\dot{W}$. Under the given conditions, the optimal design values using the PSA are $T_{h,N} = 38$ °C and $UA_H/$

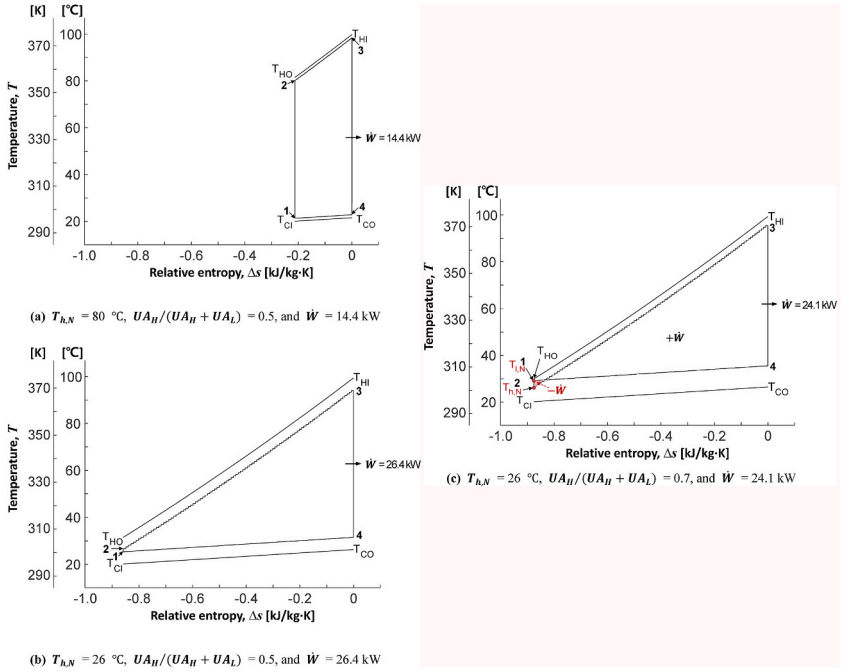

Fig. 5. None-optimization cycles on a T-s diagram.

$(UA_H + UA_L) = 0.5$, with an output $\dot{W}$ of 27.55 kW. The cycle T-s diagram at the optimum design point is shown in Fig. 7, and the area surrounded by the closed curve represents the output $\dot{W}$. The area of the cycle in Fig. 7 with the highest output power is wider compared to that of Fig. 5.

Ondrechen et al. [9] observed that, under ideal conditions, the maximum output of the sequential Carnot cycles can be obtained until the heat of the heat source is fully used (in other words, until the temperature of the heat source reaches the inlet temperature of the heat sink). But, as in practice, when the heat transfer area and the heat capacity of the heat sink are finite, there is an optimum $T_{h,N}$. In other words, maximizing the heat absorbed rate $\dot{Q}_H$ does not always maximize the output.

Fig. 8 (a) and 8 (b) show the highest power output for the two heat sink flow rates $\dot{m}_L$ as a function of $(UA_H + UA_L)$. Fig. 8 (c) shows $\Delta T_{min,H}$ (the minimum temperature difference between the cycle and the heat source) and $T_{h,N}$ as a function of $(UA_H + UA_L)$, and the optimal design points.

When the size of heat exchanger $(UA_H + UA_L)$ is 10, 50, and 200, the cycle is placed at the top of Fig. 8 (a) and 8 (b) to maximize the power with the optimized conditions. As $(UA_H + UA_L)$ increases, the performance is improved; the temperature of the working fluid in the cycle is closer to that of the heat source and sink, and the finite temperature difference (irreversible, $\Delta T_{min,H}$, $\Delta T_{min,L}$) decreases. Comparing the cycles in Fig. 8 (a) and 8 (b), when the flow rate of heat sink decreases, the $T_{l,1}$ (T_4) increases, and the power decreases. In the upper graph of Fig. 8 (c), when $(UA_H + UA_L)$ increases, heat received from the heat source increases, so the optimum $T_{h,N}$ (T_2) decreases. As the heat sink flow rate increases and $(UA_H + UA_L)$ increases, the optimum compressor outlet temperature ($T_{h,N}$) decreases. It is therefore clear that it is advantageous in terms of output to design a cycle so that the heat absorbed rate $\dot{Q}_H$ increases with the available heat transfer area and the amount of cooling water $\dot{m}_L$.

In Fig. 8 (c) and 8 (d), the change of the cycle shape and power is derived when the size of heat exchanger $(UA_H + UA_L)$ is 50, and 100. The lower compressor outlet temperature $T_{h,N}$ is, the closer it is to a trilateral cycle and the power is expected to increase. However, in reality the finite temperature difference $\Delta T_{min,H}$ increases and the area decreases, resulting in a decrease in the output. The performance of cycles (2) and (5) representing the optimal $T_{h,N}$ and $\Delta T_{min,H}$ is the best. Consistent with the previous paragraph and compared to cycles (4)–(6), cycles (1)–(3) have a larger overall heat transfer coefficient, which decreases the minimum temperature difference between the cycle and heat source and increases the power.

The $\Delta T_{min,H}$ at the optimum design point decreases with increasing $(UA_H + UA_L)$ and decreasing heat sink flow rate. $\Delta T_{min,H}$ can be thought of as the concept of the nominal size of the heat exchanger. For example, considering the typical value of 5 °C as indicated by the dotted line in Fig. 8, when the heat sink flow rate ($\dot{m}_L$) is 3 or 10 kg/s, it can be expected to achieve a peak output of approximately 22.5 or 26.8 kW, respectively. Meanwhile, the optimum $UA_H/(UA_H + UA_L)$ obtained under the calculation conditions of this study is always 0.5 regardless of the $(UA_H + UA_L)$ or heat sink flow rate $\dot{m}_L$ [4].

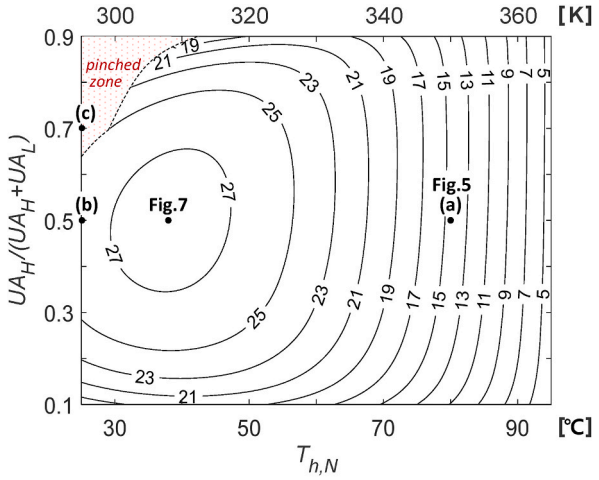

Fig. 6. Power contour map with design variables change ($\dot{W}$, [kW]).

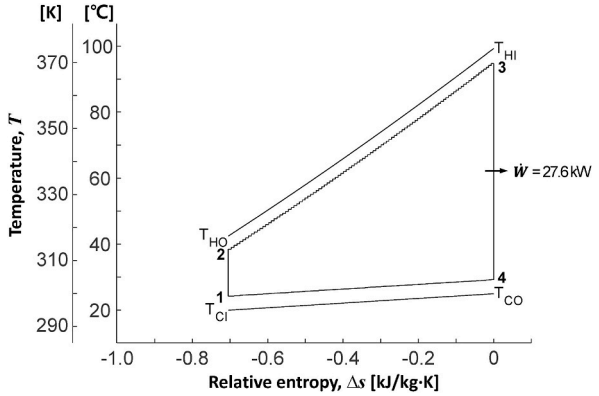

Fig. 7. Optimized sequential Carnot cycles on a T-s diagram.

In Fig. 8 (d), it was mentioned that when the $(UA_H + UA_L)$ is constant, the maximum power is not derived just because the cycle approaches the trilateral shape. However, as can be seem in Fig. 8 (a) and 8 (b), when the $(UA_H + UA_L)$ increases with the optimal design values, it approaches the trilateral cycle shown in Fig. 9. As the $(UA_H + UA_L)$ approaches infinity, it converges to $\Delta T_{min} = 0$, which means that the irreversibility of the heat exchanger is zero.

In summary, as the $(UA_H + UA_L)$ increases, the temperature difference between the cycle and heat source decreases, $T_{h,N}$ $(= T_2)$ approaches T_1, and finally the cycle forms an ideal trilateral cycle and the power of the heat engine is maximized when $(UA_H + UA_L)$ is close to infinity.

5. Conclusion

The trade-off between thermal efficiency (η_{th}) and power capacity ($\dot{W}$) of a cycle is discussed first. Those performance indexes of a heat engine can be selected separately depending on what aspects are considered to be important, such as the type of heat source, or the circulation of the working fluid. In this study, the theoretical maximum power of a heat engine operating between a heat source of 100 $°C$ and a heat sink of 20 $°C$ is calculated using the sequential Carnot cycle model. As the temperature and the flow rate of the heat source (heat capacity) are fixed, both are set as boundary conditions. The power of the heat engine is maximized by using a PSA to find the optimal combination of the two design variables which are compressor exit temperature and evaporator size ratio. Optimal design variables with changes in the overall heat transfer coefficient $(UA_H + UA_L)$ are considered. As a result, the following conclusions are obtained.

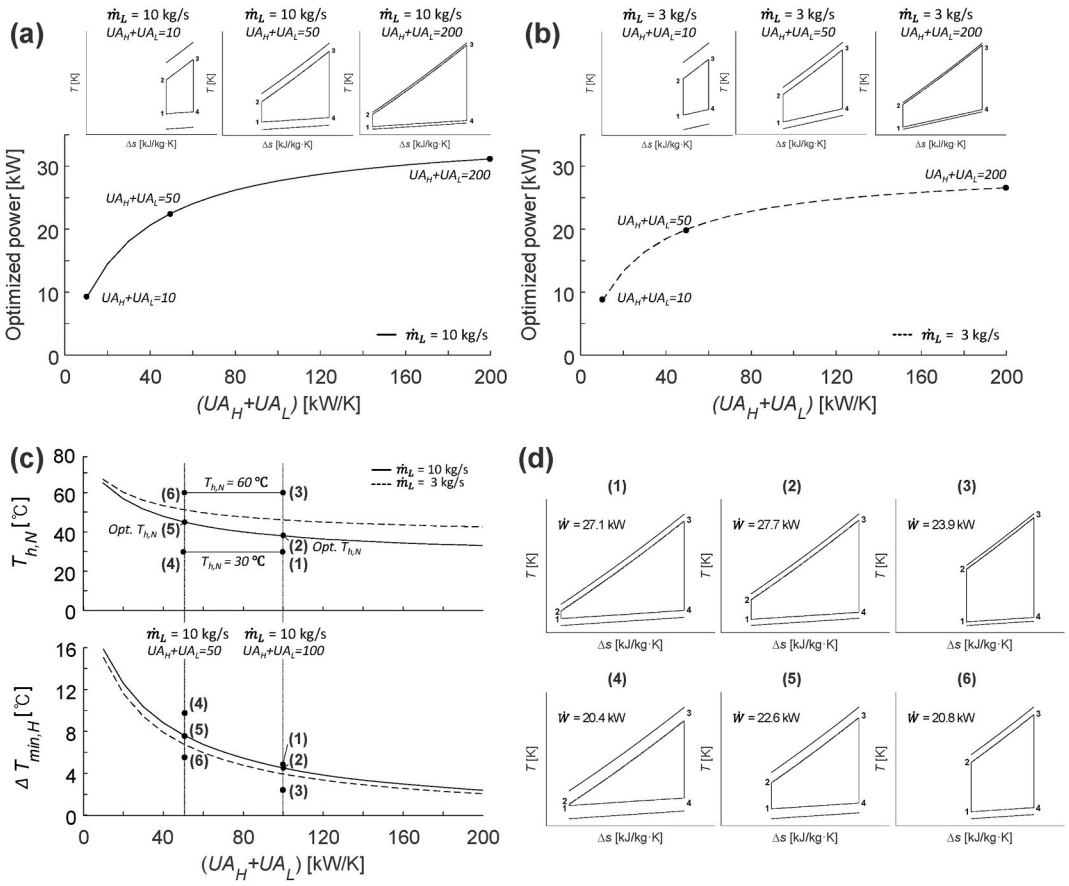

Fig. 8. Optimized power, $\Delta T_{min,H}$, and $T_{h,N}$ with $(UA_H + UA_L)$ change.

(1) When the cooling water flow rate is between 3 and 10 times the heat source flow rate, and the minimum temperature difference in the heat exchanger in the high-temperature part is 5 $^\circ C$, the theoretical maximum power per unit flow rate of heat source that can be obtained using a heat engine is between approximately 22 and 26 kW/(kg/s).

(2) The first design variable of this study, $T_{h,N}$, is the evaporator inlet temperature of the sequential Carnot cycle. There is an optimal value for $T_{h,N}$ to maximize the output. In other words, designing a lower $T_{h,N}$ to maximize the heat absorbed rate $\dot{Q}_H$ does not always maximize the output. However, the larger the size of the heating area and amount of cooling water available, the lower the optimal $T_{h,N}$ for maximizing the output.

(3) The second design variable of this study, the $UA_H/(UA_H + UA_L)$, is the evaporator size ratio that related cost of cycle design. The optimal value of $UA_H/(UA_H + UA_L)$ for maximizing the output is always 0.5 under the calculation conditions of this study.

(4) If the cycle is designed by lowering $T_{h,N}$, it gets closer to the trilateral cycle, but it does not mean that the maximum power is obtained because the minimum temperature difference between the heat source and the cycle, which represents irreversibility, increases. However, in the case of an optimal cycle in which power is maximized in a heat exchanger of fixed size, the shape of the cycle tends to approach the trilateral cycle because $T_{h,N}$ is lower and the minimum temperature difference is smaller as $(UA_H + UA_L)$ increases. In theory, an ideal trilateral cycle appears when the heat exchanger is infinitely big ($(UA_H + UA_L)$ is closer to infinity).

Author statement

Soyeon KIM: Investigation, Writing-Original draft preparation, Writing-Revised draft preparation, **Young-jin BAIK**: Formal analysis, Conceptualization, **Minsung KIM**: Supervision, Funding acquisition, Writing-Review & editing.

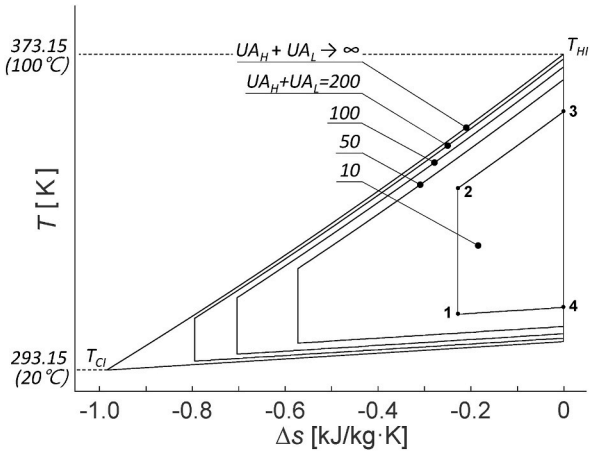

Fig. 9. Optimized power cycle varies with.($UA_H + UA_L$)

Declaration of competing interest

The authors declare that they have no known competing financial interests or personal relationships that could have appeared to influence the work reported in this paper.

Acknowledgements

This research was supported by a Chung-Ang University Graduate Research Scholarship in 2021. This research was also supported by the Korea Environmental Industry and Technology Institute (KEITI No. 2020003060005) and by the Korea Institute of Energy Technology Evaluation and Planning (KETEP No. 20202020900290). The authors appreciate their support.

References

[1] R. Bertani, Geothermal power generation in the world 2010-2014 update report, Geothermics 60 (2016) 31–43, https://doi.org/10.1016/j.geothermics.2015.11.003.
[2] L. Garcia-Rodrigues, J. Blanco-Galvez, Solar-heated Rankine cycles for water and electricity production; POWERSOL project, Desalination 212 (1–3) (2007) 311–318, https://doi.org/10.1016/j.desal.2006.08.015.
[3] H.T. Odum, Emergy evaluation of an OTEC electrical power system, Energy 25 (4) (2000) 389–393, https://doi.org/10.1016/S0360-5442(99)00076-6.
[4] Y.J. Baik, M. Kim, K.C. Chang, Y.S. Lee, H.S. Ra, Power maximization of a heat engine between the heat source and sink with finite heat capacity rates, Korean J. Air-Cond. Refrig. Eng. 23 (8) (2011) 556–561, https://doi.org/10.6110/KJACR.2011.23.8.556.
[5] K. Wang, Y.L. He, Thermodynamic analysis and optimization of a molten salt solar power tower integrated with a recompression supercritical CO2 Brayton cycle based on integrated modeling, Energy Convers. Manag. 135 (2017) 336–350, https://doi.org/10.1016/j.enconman.2016.12.085.
[6] J.D. Osorio, R. Hovsapian, J.C. Ordonez, Dynamic analysis of concentrated solar supercritical CO2-based power generation closed-loop cycle, Appl. Therm. Eng. 93 (2016) 920–934, https://doi.org/10.1016/j.applthermaleng.2015.10.039.
[7] E.K. Levy, X. Wang, C. Pan, C.E. Romero, C.R. Maya, Use of hot supercritical CO2 produced from a geothermal reservoir to generate electric power in a gas turbine power generation system, J. CO2 Util. 23 (2018) 20–28, https://doi.org/10.1016/j.jcou.2017.11.001.
[8] S.I. Na, M.S. Kim, Y.J. Baik, M. Kim, Optimal allocation of heat exchangers in a Supercritical carbon dioxide power cycle for waste cycle for waste heat recovery, Energy Convers. Manag. 199 (2019) 112002, https://doi.org/10.1016/j.enconman.2019.112002.
[9] M.J. Ondrechen, B. Anderson, M. Mozurkewich, R. Berry, Maximum work from a finite reservoir by seqential Carnot cycles, Am. J. Phys. 49 (7) (1981) 681–685, https://doi.org/10.1119/1.12426.
[10] O.M. Ibrahim, S.A. Klein, J.W. Mitchell, Optimum heat power cycles for specified boundary conditions, J. Eng. Gas Turbines Power 113 (4) (1991) 514–521, https://doi.org/10.1115/1.2906271.
[11] O.M. Ibrahim, S.A. Klein, Absorption power cycles, Energy 21 (1) (1996) 1–7, https://doi.org/10.1016/0360-5442(95)00083-6.
[12] H. Park, M.S. Kim, Thermodynamics performance analysis of sequential Carnot cycles using heat source with finite heat capacity, Energy 68 (2014) 592–598, https://doi.org/10.1016/j.energy.2014.02.073.
[13] H. Park, M.S. Kim, Performance analysis of sequential Carnot cycles with finite heat sources and heat sinks and its application in organic Rankine cycles, Energy 99 (2016) 1–9, https://doi.org/10.1016/j.energy.2016.01.019.
[14] R.M. Lewis, V. Torczon, A globally convergent augmented Lagrangian pattern search algorithm for optimization with general constraints and simple bounds, SIAM J. Optim. 12 (4) (2002) 1075–1089, https://doi.org/10.1137/S1052623498339727.
[15] Global Optimization Toolbox User's Guide, The MathWorks Inc, 2020.
[16] J.Y. Heo, M.S. Kim, S. Baik, S.J. Bae, J.I. Lee, Thermodynamic study of supercritical CO2 Brayton cycle using an isothermal compressor, Appl. Energy 206 (2017) 1118–1130, https://doi.org/10.1016/j.apenergy.2017.08.081.
[17] J.K. Ham, M.S. Kim, B.S. Oh, S. Son, J. Lee, J.I. Lee, A supercritical CO2 waste heat recovery system design for a diesel generator for nuclear power plant application, Appl. Sci. 9 (24) (2019) 5382, https://doi.org/10.3390/app9245382.
[18] S.J. Zarrouk, H. Moon, Efficiency of geothermal power plants: a worldwide review, Geothermics 51 (2014) 142–153, https://doi.org/10.1016/j.geothermics.2013.11.001.
[19] S. Amicabile, J.I. Lee, D. Kum, A comprehensive design methodology of organic Rankine cycles for the waste heat recovery of automotive heavy-duty diesel engines, Appl. Therm. Eng. 87 (2015) 574–585, https://doi.org/10.1016/j.applthermaleng.2015.04.034.
[20] Y.A. Cengel, M.A. Boles, Thermodynamics: an Engineering Approach, eighth ed., McGraw-Hill, Boston, 2015.
[21] Y.J. Baik, Study on the Power Optimization of Transcritical and Subcritical Rankine Power Cycles for a Low-Grade Heat Source, Ph.D Dissertation, Korea Advanced Institute of Science and Technology, 2011.

[22] S.J. Kim, P.S. Jung, S.T. Ro, Analysis of a heat engine with the irreversibility by the heat transfer, Trans. Korean Soc. Mech. 8 (6) (1984) 564–568. http://www.dbpia.co.kr/journal/articleDetail?nodeId=NODE00344321.
[23] S.J. Kim, M.S. Kim, M. Kim, Parametric study and optimization of closed Brayton power cycle considering the charge amount of working fluid, Energy 198 (2020) 117353, https://doi.org/10.1016/j.energy.2020.117353.
[24] I.K. Smith, Matching and work ratio in elementary thermal power plant theory, Proc. IME J. Power Energy 206 (4) (1992) 257–262, https://doi.org/10.1243/PIME_PROC_1992_206_042_02.
[25] J. Fischer, Comparison of trilateral cycles and organic Rankine cycles, Energy 36 (10) (2011) 6208–6219, https://doi.org/10.1016/j.energy.2011.07.041.
[26] M. Aneke, B. Agnew, C. Underwood, Performance analysis of the China binary geothermal power plant, Appl. Therm. Eng. 31 (10) (2011) 1825–1832, https://doi.org/10.1016/j.applthermaleng.2011.02.028.
[27] H. Milcak, M. Mirolli, H. Hjartarson, O. Húsavíkur, M. Ralph, Notes from the North : a report on the debut year of the 2 MW Kalina cycle geothermal power plant in Húsavik, Iceland, Trans. Geoth. Resour. Counc. 26 (2002) 22–25. https://www.geothermal-library.org/index.php?mode=pubs&action=view&record=1019686.
[28] C. Audet, J.E. Dennis, Jr, Analysis of generalized pattern searches, SIAM J. Optim. 13 (3) (2002) 889–903, https://doi.org/10.1137/S1052623400378742.